



KEK preprint 2001-117  
Belle preprint 2001-14

## Observation of Color-suppressed $\bar{B}^0 \rightarrow D^0\pi^0$ , $D^{*0}\pi^0$ , $D^0\eta$ , and $D^0\omega$ Decays\*

K. Abe<sup>9</sup>, K. Abe<sup>36</sup>, R. Abe<sup>27</sup>, I. Adachi<sup>9</sup>, Byoung Sup Ahn<sup>15</sup>, H. Aihara<sup>38</sup>, M. Akatsu<sup>20</sup>, Y. Asano<sup>42</sup>, T. Aso<sup>41</sup>, V. Aulchenko<sup>2</sup>, T. Aushev<sup>13</sup>, A. M. Bakich<sup>34</sup>, E. Banas<sup>25</sup>, S. Behari<sup>9</sup>, P. K. Behera<sup>43</sup>, A. Bondar<sup>2</sup>, A. Bozek<sup>25</sup>, T. E. Browder<sup>8</sup>, B. C. K. Casey<sup>8</sup>, P. Chang<sup>24</sup>, Y. Chao<sup>24</sup>, K. F. Chen<sup>24</sup>, B. G. Cheon<sup>33</sup>, R. Chistov<sup>13</sup>, S.-K. Choi<sup>7</sup>, Y. Choi<sup>33</sup>, L. Y. Dong<sup>12</sup>, J. Dragic<sup>18</sup>, A. Drutskoy<sup>13</sup>, S. Eidelman<sup>2</sup>, Y. Enari<sup>20</sup>, F. Fang<sup>8</sup>, H. Fujii<sup>9</sup>, M. Fukushima<sup>11</sup>, N. Gabyshev<sup>9</sup>, A. Garmash<sup>2,9</sup>, T. Gershon<sup>9</sup>, A. Gordon<sup>18</sup>, K. Gotow<sup>44</sup>, R. Guo<sup>22</sup>, J. Haba<sup>9</sup>, H. Hamasaki<sup>9</sup>, F. Handa<sup>37</sup>, K. Hara<sup>29</sup>, T. Hara<sup>29</sup>, N. C. Hastings<sup>18</sup>, H. Hayashii<sup>21</sup>, M. Hazumi<sup>29</sup>, E. M. Heenan<sup>18</sup>, I. Higuchi<sup>37</sup>, T. Higuchi<sup>38</sup>, H. Hirano<sup>40</sup>, T. Hojo<sup>29</sup>, T. Hokuue<sup>20</sup>, K. Hoshina<sup>40</sup>, S. R. Hou<sup>24</sup>, W.-S. Hou<sup>24</sup>, S.-C. Hsu<sup>24</sup>, H.-C. Huang<sup>24</sup>, Y. Igarashi<sup>9</sup>, T. Iijima<sup>9</sup>, H. Ikeda<sup>9</sup>, K. Inami<sup>20</sup>, A. Ishikawa<sup>20</sup>, H. Ishino<sup>39</sup>, R. Itoh<sup>9</sup>, H. Iwasaki<sup>9</sup>, Y. Iwasaki<sup>9</sup>, D. J. Jackson<sup>29</sup>, H. K. Jang<sup>32</sup>, H. Kakuno<sup>39</sup>, J. Kaneko<sup>39</sup>, J. H. Kang<sup>46</sup>, J. S. Kang<sup>15</sup>, P. Kapusta<sup>25</sup>, N. Katayama<sup>9</sup>, H. Kawai<sup>3</sup>, H. Kawai<sup>38</sup>, N. Kawamura<sup>1</sup>, T. Kawasaki<sup>27</sup>, H. Kichimi<sup>9</sup>, D. W. Kim<sup>33</sup>, Heejong Kim<sup>46</sup>, H. J. Kim<sup>46</sup>, H. O. Kim<sup>33</sup>, Hyunwoo Kim<sup>15</sup>, S. K. Kim<sup>32</sup>, T. H. Kim<sup>46</sup>, K. Kinoshita<sup>5</sup>, S. Kobayashi<sup>31</sup>, H. Konishi<sup>40</sup>, P. Krokovny<sup>2</sup>, R. Kulasiri<sup>5</sup>, S. Kumar<sup>30</sup>, A. Kuzmin<sup>2</sup>, Y.-J. Kwon<sup>46</sup>, J. S. Lange<sup>6</sup>, S. H. Lee<sup>32</sup>, D. Liventsev<sup>13</sup>, R.-S. Lu<sup>24</sup>, T. Matsubara<sup>38</sup>, S. Matsumoto<sup>4</sup>, T. Matsumoto<sup>20</sup>, Y. Mikami<sup>37</sup>, K. Miyabayashi<sup>21</sup>, H. Miyake<sup>29</sup>, H. Miyata<sup>27</sup>, G. R. Moloney<sup>18</sup>, G. F. Moorhead<sup>18</sup>, S. Mori<sup>42</sup>, T. Mori<sup>4</sup>, A. Murakami<sup>31</sup>, T. Nagamine<sup>37</sup>, Y. Nagasaka<sup>10</sup>, Y. Nagashima<sup>29</sup>, T. Nakadaira<sup>38</sup>, E. Nakano<sup>28</sup>, M. Nakao<sup>9</sup>, J. W. Nam<sup>33</sup>, Z. Natkaniec<sup>25</sup>, K. Neichi<sup>36</sup>, S. Nishida<sup>16</sup>, O. Nitoh<sup>40</sup>, S. Noguchi<sup>21</sup>, T. Nozaki<sup>9</sup>, S. Ogawa<sup>35</sup>, T. Ohshima<sup>20</sup>, T. Okabe<sup>20</sup>, S. Okuno<sup>14</sup>, S. L. Olsen<sup>8</sup>, W. Ostrowicz<sup>25</sup>, H. Ozaki<sup>9</sup>, P. Pakhlov<sup>13</sup>, H. Palka<sup>25</sup>, C. S. Park<sup>32</sup>, C. W. Park<sup>15</sup>, H. Park<sup>17</sup>, K. S. Park<sup>33</sup>, L. S. Peak<sup>34</sup>, M. Peters<sup>8</sup>, L. E. Piilonen<sup>44</sup>, J. L. Rodriguez<sup>8</sup>, N. Root<sup>2</sup>, M. Rozanska<sup>25</sup>, K. Rybicki<sup>25</sup>, J. Ryuko<sup>29</sup>, H. Sagawa<sup>9</sup>, Y. Sakai<sup>9</sup>, H. Sakamoto<sup>16</sup>, M. Satpathy<sup>43</sup>, A. Satpathy<sup>9,5</sup>, S. Schrenk<sup>5</sup>, S. Semenov<sup>13</sup>, K. Senyo<sup>20</sup>, M. E. Sevior<sup>18</sup>, H. Shibuya<sup>35</sup>, B. Shwartz<sup>2</sup>, A. Sidorov<sup>2</sup>, S. Stanic<sup>42</sup>, A. Sugi<sup>20</sup>, A. Sugiyama<sup>20</sup>, K. Sumisawa<sup>9</sup>, T. Sumiyoshi<sup>9</sup>, K. Suzuki<sup>3</sup>, S. Suzuki<sup>45</sup>, S. Y. Suzuki<sup>9</sup>, S. K. Swain<sup>8</sup>, T. Takahashi<sup>28</sup>, F. Takasaki<sup>9</sup>, M. Takita<sup>29</sup>, K. Tamai<sup>9</sup>, N. Tamura<sup>27</sup>, J. Tanaka<sup>38</sup>, M. Tanaka<sup>9</sup>, Y. Tanaka<sup>19</sup>, G. N. Taylor<sup>18</sup>, Y. Teramoto<sup>28</sup>, M. Tomoto<sup>9</sup>, T. Tomura<sup>38</sup>, S. N. Tovey<sup>18</sup>, K. Trabelsi<sup>8</sup>, T. Tsuboyama<sup>9</sup>, T. Tsukamoto<sup>9</sup>, S. Uehara<sup>9</sup>, K. Ueno<sup>24</sup>,

---

\*to appear in PRL

Y. Unno<sup>3</sup>, S. Uno<sup>9</sup>, Y. Ushiroda<sup>9</sup>, K. E. Varvell<sup>34</sup>, C. C. Wang<sup>24</sup>, C. H. Wang<sup>23</sup>,  
J. G. Wang<sup>44</sup>, M.-Z. Wang<sup>24</sup>, Y. Watanabe<sup>39</sup>, E. Won<sup>32</sup>, B. D. Yabsley<sup>9</sup>, Y. Yamada<sup>9</sup>,  
M. Yamaga<sup>37</sup>, A. Yamaguchi<sup>37</sup>, H. Yamamoto<sup>37</sup>, Y. Yamashita<sup>26</sup>, M. Yamauchi<sup>9</sup>,  
S. Yanaka<sup>39</sup>, J. Yashima<sup>9</sup>, M. Yokoyama<sup>38</sup>, K. Yoshida<sup>20</sup>, Y. Yuan<sup>12</sup>, Y. Yusa<sup>37</sup>,  
C. C. Zhang<sup>12</sup>, J. Zhang<sup>42</sup>, Y. Zheng<sup>8</sup>, V. Zhilich<sup>2</sup>, and D. Žontar<sup>42</sup>

## Belle Collaboration

- <sup>1</sup>Aomori University, Aomori  
<sup>2</sup>Budker Institute of Nuclear Physics, Novosibirsk  
<sup>3</sup>Chiba University, Chiba  
<sup>4</sup>Chuo University, Tokyo  
<sup>5</sup>University of Cincinnati, Cincinnati OH  
<sup>6</sup>University of Frankfurt, Frankfurt  
<sup>7</sup>Gyeongsang National University, Chinju  
<sup>8</sup>University of Hawaii, Honolulu HI  
<sup>9</sup>High Energy Accelerator Research Organization (KEK), Tsukuba  
<sup>10</sup>Hiroshima Institute of Technology, Hiroshima  
<sup>11</sup>Institute for Cosmic Ray Research, University of Tokyo, Tokyo  
<sup>12</sup>Institute of High Energy Physics, Chinese Academy of Sciences, Beijing  
<sup>13</sup>Institute for Theoretical and Experimental Physics, Moscow  
<sup>14</sup>Kanagawa University, Yokohama  
<sup>15</sup>Korea University, Seoul  
<sup>16</sup>Kyoto University, Kyoto  
<sup>17</sup>Kyungpook National University, Taegu  
<sup>18</sup>University of Melbourne, Victoria  
<sup>19</sup>Nagasaki Institute of Applied Science, Nagasaki  
<sup>20</sup>Nagoya University, Nagoya  
<sup>21</sup>Nara Women's University, Nara  
<sup>22</sup>National Kaohsiung Normal University, Kaohsiung  
<sup>23</sup>National Lien-Ho Institute of Technology, Miao Li  
<sup>24</sup>National Taiwan University, Taipei  
<sup>25</sup>H. Niewodniczanski Institute of Nuclear Physics, Krakow  
<sup>26</sup>Nihon Dental College, Niigata  
<sup>27</sup>Niigata University, Niigata  
<sup>28</sup>Osaka City University, Osaka  
<sup>29</sup>Osaka University, Osaka  
<sup>30</sup>Panjab University, Chandigarh  
<sup>31</sup>Saga University, Saga  
<sup>32</sup>Seoul National University, Seoul  
<sup>33</sup>Sungkyunkwan University, Suwon  
<sup>34</sup>University of Sydney, Sydney NSW  
<sup>35</sup>Toho University, Funabashi  
<sup>36</sup>Tohoku Gakuin University, Tagajo  
<sup>37</sup>Tohoku University, Sendai  
<sup>38</sup>University of Tokyo, Tokyo

<sup>39</sup>Tokyo Institute of Technology, Tokyo

<sup>40</sup>Tokyo University of Agriculture and Technology, Tokyo

<sup>41</sup>Toyama National College of Maritime Technology, Toyama

<sup>42</sup>University of Tsukuba, Tsukuba

<sup>43</sup>Utkal University, Bhubaneswer

<sup>44</sup>Virginia Polytechnic Institute and State University, Blacksburg VA

<sup>45</sup>Yokkaichi University, Yokkaichi

<sup>46</sup>Yonsei University, Seoul

(October 31, 2018)

## Abstract

We report the first observation of color-suppressed  $\bar{B}^0 \rightarrow D^0\pi^0$ ,  $D^{*0}\pi^0$ ,  $D^0\eta$ , and  $D^0\omega$  decays and evidence for  $\bar{B}^0 \rightarrow D^{*0}\eta$  and  $D^{*0}\omega$ . The branching fractions are found to be  $\mathcal{B}(\bar{B}^0 \rightarrow D^0\pi^0) = (3.1 \pm 0.4 \pm 0.5) \times 10^{-4}$ ,  $\mathcal{B}(\bar{B}^0 \rightarrow D^{*0}\pi^0) = (2.7^{+0.8}_{-0.7} \ ^{+0.5}_{-0.6}) \times 10^{-4}$ ,  $\mathcal{B}(\bar{B}^0 \rightarrow D^0\eta) = (1.4^{+0.5}_{-0.4} \pm 0.3) \times 10^{-4}$ ,  $\mathcal{B}(\bar{B}^0 \rightarrow D^0\omega) = (1.8 \pm 0.5 \ ^{+0.4}_{-0.3}) \times 10^{-4}$ , and we set 90% confidence level upper limits of  $\mathcal{B}(\bar{B}^0 \rightarrow D^{*0}\eta) < 4.6 \times 10^{-4}$  and  $\mathcal{B}(\bar{B}^0 \rightarrow D^{*0}\omega) < 7.9 \times 10^{-4}$ . The analysis is based on a data sample of  $21.3 \text{ fb}^{-1}$  collected at the  $\Upsilon(4S)$  resonance by the Belle detector at the KEKB  $e^+e^-$  collider.

PACS numbers: 13.25.Hw, 14.40.Nd

Decay modes such as  $\bar{B}^0 \rightarrow D^{(*)+}\pi^-$  were amongst the first  $B$  meson decays to be fully reconstructed. However, the  $\bar{B}^0 \rightarrow D^{(*)0}h^0$  decay modes, where  $h^0$  represents a light neutral meson, have not been observed to date. A recent search by the CLEO Collaboration [1] yielded only upper limits. As shown in Fig. 1, these decays are expected to proceed via an internal spectator diagram and be suppressed relative to decays proceeding via the external spectator diagram, since the color of the  $\bar{u}$  antiquark produced by the weak current must complement the color of the  $c$  quark. The contribution of the  $W$ -exchange diagram is usually assumed to be negligible [2]. Studies of such color-suppressed decay modes are useful for testing models of hadronic  $B$  meson decay and provide information on final-state interactions. Final state interactions, if also present in  $B$  decays to charmless modes, could have significant impact on  $CP$  violating rate asymmetries [3]. Furthermore, studies of  $\bar{B}^0 \rightarrow D^{(*)0}h^0$  where the  $D^0$  decays to a  $CP$  eigenstate will provide access to the  $CP$  violation parameter  $\sin 2\phi_1$  in  $b \rightarrow c\bar{u}d$  processes [4]. Thus, measuring the strength of color-suppressed modes can have profound implications on  $B$  physics and  $CP$  violation.

In this paper, we report on a search for the color-suppressed  $\bar{B}^0 \rightarrow D^0h^0$  and  $D^{*0}h^0$  [5] decays, where the neutral meson  $h^0$  is either a  $\pi^0$ ,  $\eta$ , or  $\omega$ . We make first observations of the modes  $\bar{B}^0 \rightarrow D^0\pi^0$ ,  $D^{*0}\pi^0$ ,  $D^0\eta$ , and  $D^0\omega$  and find evidence for the modes  $\bar{B}^0 \rightarrow D^{*0}\eta$  and  $D^{*0}\omega$ . The data used in this analysis were collected with the Belle detector [6] at KEKB [7], a double storage ring that collides 8 GeV electrons with 3.5 GeV positrons with a 22 mrad crossing angle. The data sample corresponds to an integrated luminosity of  $21.3 \text{ fb}^{-1}$  at the  $\Upsilon(4S)$  resonance, which contains 23.1 million  $B\bar{B}$  pairs, and  $2.3 \text{ fb}^{-1}$  taken 60 MeV below the resonance.

Belle is a general-purpose detector with a 1.5 T superconducting solenoid magnet. Charged particle tracking, covering 92% of the total center-of-mass (CM) solid angle, is provided by the Silicon Vertex Detector (SVD) consisting of three concentric layers of double-sided silicon strip detectors and a 50-layer Central Drift Chamber (CDC). Charged hadrons are distinguished by combining the responses from an array of Silica Aerogel Čerenkov Counters (ACC), a Time of Flight Counter system (TOF), and  $dE/dx$  measurements in the CDC. The combined response provides  $K/\pi$  separation of at least  $2.5\sigma$  for laboratory momenta up to  $3.5 \text{ GeV}/c$ . Photons and electrons are detected in an array of 8736 CsI(Tl) crystals (ECL) located inside the magnetic field and covering the entire solid angle of the charged particle tracking system. The 1.5 T magnetic field is returned via an iron yoke, instrumented to detect muons and  $K_L$  mesons (KLM). The KLM consists of alternating layers of resistive plate chambers and 4.7 cm thick steel plates.

We reconstruct light neutral mesons  $h^0$  using the  $\pi^0 \rightarrow \gamma\gamma$ ,  $\eta \rightarrow \gamma\gamma$ ,  $\eta \rightarrow \pi^+\pi^-\pi^0$  and  $\omega \rightarrow \pi^+\pi^-\pi^0$  decay channels. Charged tracks are required to have impact parameters that are within  $\pm 5$  cm of the interaction point along the positron beam axis and 1 cm in the transverse plane. We reject tracks that are consistent with being electrons or muons. The remaining tracks are identified as pions or kaons according to a kaon to pion likelihood ratio. Candidate  $\pi^0$  mesons are reconstructed from pairs of photons in the ECL if the  $\gamma$  pairs have invariant mass inside a  $\pm 3\sigma$  ( $\sigma = 5.4 \text{ MeV}/c^2$ ) mass window around the  $\pi^0$  peak. The  $\pi^0$  daughter photons are required to have energies greater than 50 MeV. The  $\pi^0$ s are then constrained to the nominal  $\pi^0$  mass [8]. Candidate  $\eta$  mesons are required to have invariant masses within  $\pm 2.5\sigma$  of the  $\eta$  peak, where  $\sigma$  is  $10.6 \text{ MeV}/c^2$  and  $3.4 \text{ MeV}/c^2$  for the  $\gamma\gamma$  and  $\pi^+\pi^-\pi^0$  modes, respectively. For the  $\pi^+\pi^-\pi^0$  mode, the  $\pi^+\pi^-$  pair is constrained to a vertex.

Both photons from the  $\eta \rightarrow \gamma\gamma$  mode are required to have  $E_\gamma > 100$  MeV and the energy asymmetry of the daughter photons,  $\frac{|E_{\gamma_1} - E_{\gamma_2}|}{E_{\gamma_1} + E_{\gamma_2}}$ , is required to be less than 0.8. We remove  $\eta$  candidates if either of the daughter photons can be combined with any other photon with  $E_\gamma > 100$  MeV to form a  $\pi^0$  candidate. The  $\eta$  candidates are further constrained to the known  $\eta$  mass [8]. Candidate  $\omega$  mesons are constructed from  $\pi^+\pi^-\pi^0$  combinations where the  $\pi^+\pi^-$  pair must form a vertex, and the CM momentum of the  $\pi^0$  is required to be greater than 350 MeV/c to reduce the large combinatorial background from low energy photons. The invariant mass of the  $\pi^+\pi^-\pi^0$  combination is required to be within  $\pm 30$  MeV/c<sup>2</sup> of the nominal  $\omega$  mass [8] (the natural width of the  $\omega$  is 8.9 MeV/c<sup>2</sup>).

We reconstruct  $D^0$  mesons in the  $D^0 \rightarrow K^-\pi^+$ ,  $K^-\pi^+\pi^0$ , and  $K^-\pi^+\pi^-\pi^+$  decay modes. The CM momentum of the  $\pi^0$  from  $D^0 \rightarrow K^-\pi^+\pi^0$  decay is required to be greater than 300 MeV/c. The invariant mass of the  $D^0$  candidate is required to be within  $\pm 2.5\sigma$  of the measured  $D^0$  mass where  $\sigma$ , the  $D^0$  mass resolution, varies between 5.5 and 13 MeV/c<sup>2</sup> depending on the decay mode. A mass and vertex-constrained kinematic fit is then performed on the  $D^0$  candidates.  $D^{*0}$  candidates are reconstructed in the  $D^{*0} \rightarrow D^0\pi^0$  decay mode; the minimum photon energy requirement is reduced to 20 MeV for this case. The mass difference,  $\delta m = M(D^0\pi^0) - M(D^0)$ , is required to be within  $\pm 2.5\sigma$  ( $\sigma = 0.82$  MeV/c<sup>2</sup>) of its nominal value.

We combine  $D^0$ s or  $D^{*0}$ s with  $h^0$  meson candidates to form  $\bar{B}^0$  candidates. Two kinematic variables are used to identify signal candidates, the beam-constrained mass  $M_{bc} = \sqrt{(E_{\text{beam}}^{\text{CM}})^2 - (p_B^{\text{CM}})^2}$  and the energy difference  $\Delta E = E_B^{\text{CM}} - E_{\text{beam}}^{\text{CM}}$ , where  $E_B^{\text{CM}}$  and  $p_B^{\text{CM}}$  are the CM energy and momentum of the  $\bar{B}^0$  candidate, and  $E_{\text{beam}}^{\text{CM}} = \sqrt{s}/2 = 5.29$  GeV. The typical  $M_{bc}$  resolution is 3 MeV/c<sup>2</sup>; the  $\Delta E$  resolution ranges from 17 to 35 MeV, depending on the decay mode. When more than one  $\bar{B}^0$  candidate is found in an event, the candidate with the minimum  $\chi^2$  is chosen, where  $\chi^2 = \chi_{D^0}^2 + \chi_{h^0}^2 (+\chi_{\delta m}^2)$ . Here  $\chi_{D^0}^2$  is from the kinematic fit to the  $D^0$ ,  $\chi_{h^0}^2$  is from the kinematic fit to the  $h^0$  for the  $\pi^0$  or the  $\eta$ , while  $\chi_{h^0}^2 = (\Delta(M_\omega)/\sigma(M_\omega))^2$  for the  $\omega$ . Here  $\Delta(M_\omega)$  is the mass difference between measured and nominal mass values and  $\sigma(M_\omega)$  is the measured resolution. For the  $D^{*0}h^0$  modes,  $\chi_{\delta m}^2$ , defined as  $(\Delta(\delta m)/\sigma(\delta m))^2$ , is included in the best candidate selection.

The background from continuum  $e^+e^- \rightarrow q\bar{q}$  production is suppressed in the following way. We form a Fisher discriminant [9] containing seven variables that quantify event topology. The Fisher variables include the angle between the thrust axis [10] of the  $B$  candidate and the thrust axis of the rest of the event ( $\cos\theta_T$ ), the  $S_\perp$  variable [11], and five modified [12] Fox-Wolfram moments [13]. In the  $D^{*0}\pi^0$  and  $D^0\omega$  modes, helicity provides additional discrimination. For the  $D^{*0}\pi^0$  mode, we define  $\mathcal{H}_{D^{*0}}$  as the cosine of the angle between the  $D^{*0}$  flight direction and the direction of the  $\pi^0$  in the  $D^{*0}$  rest frame and require  $|\mathcal{H}_{D^{*0}}| > 0.4$ . For the  $D^0\omega$  mode, we define  $\mathcal{H}_\omega$  as the cosine of the angle between the  $B$  flight direction and the normal to the  $\omega$  decay plane in the  $\omega$  rest frame. We also define a variable  $\mathcal{A}$  as the absolute value of the cross product of the two charged pion momentum vectors,  $|\vec{P}_{\pi^+} \times \vec{P}_{\pi^-}|$ , in the  $\omega$  rest frame. To suppress the  $q\bar{q}$  background, we take the  $B$  flight direction and the Fisher discriminant, and for modes with  $\omega$  mesons we include the variable  $\mathcal{A}$ . For the  $D^0\omega$  mode, we also include the variable  $\mathcal{H}_\omega$ . These variables are then combined to form signal (S) and background (BG) probability density functions (PDFs). Signal PDFs are determined using Monte Carlo (MC), and background PDFs are obtained from  $M_{bc}$  sideband data. The PDFs are multiplied to form a signal (background) likelihood

$\mathcal{L}_{S(\text{BG})}$ , and a selection is applied on the likelihood ratio  $\mathcal{L}_S/(\mathcal{L}_S + \mathcal{L}_{\text{BG}})$ . This requirement, which has a typical efficiency of 70%, removes more than 90% of the  $q\bar{q}$  background.

In addition to the  $q\bar{q}$  background, there are large background contributions from color-favored  $B \rightarrow D^{(*)}(n\pi)^-$  decays and feed-down from  $D^{*0}h^0$  to  $D^0h^0$  modes. The color-favored  $B \rightarrow D^{(*)}(n\pi)^-$  events give rise to two kinds of backgrounds: those with the same final state particles as signal events, and those with missing or extra particles. The former mimics the signal distributions in both  $M_{bc}$  and  $\Delta E$ , and selection cuts on variables other than these (discussed below) are needed to suppress these backgrounds. The backgrounds with different final state particles arise when a pion is missed or a spurious pion is added. In this case, the background events may not be distinguishable in the  $M_{bc}$  distribution if the missing or extra pion has very low momentum, but the  $\Delta E$  distribution provides a useful discriminant because of the missing pion rest-mass energy.

The  $\bar{B}^0 \rightarrow D^{*+}\rho^-$  mode can give the same final states as  $D^0\omega$  and  $D^0\eta$ . However, more than 99% of the background events are removed by the  $\omega$  and  $\eta$  mass cuts since the invariant mass of the three pions rarely falls within the  $\omega$  or  $\eta$  mass region.

The  $B^- \rightarrow D^{(*)0}\rho^-$  final state can contaminate the  $D^{(*)0}\pi^0$  mode if the  $\rho^-$  decay produces a fast  $\pi^0$ . The background events from  $D^0\rho^-$  to  $D^0\pi^0$  ( $D^{*0}\rho^-$  to  $D^{*0}\pi^0$ ) have  $\Delta E$  values that are below the signal region because of the slow  $\pi^-$  that is missed in the reconstruction. However, the signal contamination is not negligible due to the large branching fraction of  $B^- \rightarrow D^{(*)0}\rho^-$ . The  $D^0\rho^-$  mode can also cause a background to  $D^{*0}\pi^0$  if a low momentum  $\pi^0$  is used to form a  $D^{*0}$  candidate. This case is similar to the case where the final state particles are the same, and causes a few events in the signal region. About half of these events are removed by rejecting events that can be reconstructed as  $B^- \rightarrow D^{(*)0}\rho^-$ . This reduces the systematic error when fitting for the signal yields and only removes a few percent of signal events.

The  $B^- \rightarrow D^{(*)0}\rho^-$  mode can also contaminate the  $D^{(*)0}\eta$  channel if a photon from the fast  $\pi^0$  is combined with another photon to form an  $\eta$  candidate. The contributions of these backgrounds in the  $\eta$  channel, as well as the feed-across from the  $D^{(*)0}\pi^0$  mode, are minimized by the  $\pi^0$  veto described earlier.

We also check the background contributions from  $B^- \rightarrow D^{(*)0}\rho'^-$  ( $\rho'^- \rightarrow \omega\pi^-$ ) decays that have been reported recently by the CLEO Collaboration [14]. This two-body decay produces high momentum  $D^{(*)0}$ s and  $\omega$ s that may fake signal events. Monte Carlo studies indicate that the remaining background events are shifted in  $\Delta E$  by more than the mass of the missing pion and thus are distinguished from signal events by the fit to the  $\Delta E$  distribution. The  $D^0\rho'^-$  mode can also contaminate the  $D^{*0}\omega$  mode if the  $\pi^-$  from  $\rho'^-$  is replaced by a  $\pi^0$ . However, since the  $\pi^-$  from  $\rho'^-$  decay carries sizable momentum, the kinematics of the final state particles are different from that of the  $D^{*0}\omega$  signal, and the expected background is small.

The  $\Delta E$  distributions for the various  $D^{(*)0}h^0$  decays, after the application of all selection requirements and with  $M_{bc}$  between 5.27 GeV/ $c^2$  and 5.29 GeV/ $c^2$ , are shown in Fig. 2. The plots are fitted to the signal and background functions using a binned maximum likelihood. The signal shape is an empirically determined parameterization [15] with parameters obtained via MC. We observe good agreement between data and MC for the  $\Delta E$  distributions of color-favored decays such as  $D^{*+}\rho^-$  and  $D^0\rho^-$ . The background functions include a combinatorial component and a color-favored component. For the  $D^0h^0$  modes, we also include a

component for feed-down from color-suppressed  $D^{*0}h^0$  modes. The contribution from  $D^{*0}h^0$  to  $D^0h^0$  modes is found to be negligible. The combinatorial component is taken to be a first-order polynomial with a slope determined from the  $\Delta E$  shape of the  $M_{bc}$  sideband ( $5.20 \text{ GeV}/c^2 < M_{bc} < 5.26 \text{ GeV}/c^2$ ) data. The shapes of the color-favored and feed-down components are modeled by MC. The area of the feed-down component from  $D^{*0}h^0$  to  $D^0h^0$  is fixed by the obtained signal yield from  $D^{*0}h^0$  with the estimated feed-down efficiency in MC. For the  $D^{(*)0}\omega$  mode, the  $D^{(*)0}\rho'^-$  components are also fixed by MC using the measured branching fractions [14]. The normalizations of the signal and background components are free parameters.

Table I lists the signal yield, statistical significance, reconstruction efficiency, and branching fraction for each  $D^{(*)0}h^0$  mode. In addition, the estimated number of events in the region of  $-0.1 \text{ GeV} < \Delta E < 0.1 \text{ GeV}$  due to backgrounds from generic  $B\bar{B}$  decays,  $D^{*0}h^0$  feed-down, and  $q\bar{q}$  production are given. The systematic errors due to fitting are obtained by varying the parameters of the fitting functions within  $1\sigma$  of their nominal values. The change in the signal yield from each variation is added in quadrature to obtain systematic errors from the fit. These are between 5% and 15% depending on the decay mode. The statistical significance is defined as  $\sqrt{-2\ln(\mathcal{L}(0)/\mathcal{L}_{\max})}$  where  $\mathcal{L}_{\max}$  is the likelihood at the nominal signal yield and  $\mathcal{L}(0)$  is the likelihood with the signal yield fixed to zero. We observe signals for  $\bar{B}^0 \rightarrow D^0\pi^0$ ,  $D^{*0}\pi^0$ ,  $D^0\eta$ , and  $D^0\omega$  decays with more than  $4\sigma$  significance. Independent fits to the  $M_{bc}$  distributions, after subtracting  $B\bar{B}$  background, confirm these results. We find evidence for  $\bar{B}^0 \rightarrow D^{*0}\eta$  and  $D^{*0}\omega$  with more than  $3\sigma$  significance. For decay modes with significance less than  $4\sigma$ , we give 90% confidence level upper limits (UL) on the signal yields ( $N_S^{\text{UL}}$ ) from the relation  $\int_0^{N_S^{\text{UL}}} \mathcal{L}(N_S) dN_S / \int_0^\infty \mathcal{L}(N_S) dN_S = 0.9$ , where  $\mathcal{L}(N_S)$  denotes the maximum likelihood with the signal yield fixed at  $N_S$ .

The efficiencies for each mode are obtained by Monte Carlo and calibrated by a detailed study of detector performance. In particular, studies of tracking,  $\pi^0$  detection, and particle identification give systematic errors in the detection efficiencies of low momentum  $\pi^0$ , energetic  $\pi^0$ ,  $\eta$ , and  $\omega$  mesons of 10.7%, 7.3%, 9.6%, and 9.5% respectively. The systematic error on the  $D^0$  meson reconstruction efficiency is estimated to be 12.7% by comparing the observed yield of  $B^- \rightarrow D^0\pi^-$  events with the expected yield using known branching fractions [8]. A 5% systematic error on the likelihood ratio requirement is determined by applying the same procedure to the  $B^- \rightarrow D^{*0}\pi^-$  sample and comparing the effects on data and MC. The final systematic errors of the branching fractions include the errors in fitting, reconstruction efficiency, cut efficiency for background suppression, and the number of  $B\bar{B}$  pairs. Assuming the number of  $B^0\bar{B}^0$  and  $B^+B^-$  pairs to be equal, we calculate the branching fractions for various decay modes given in Table I. The branching fraction upper limits are calculated by increasing  $N_S^{\text{UL}}$  and reducing the efficiency by their systematic errors.

Our measurement of  $\mathcal{B}(\bar{B}^0 \rightarrow D^0\pi^0) = (3.1 \pm 0.4 \pm 0.5) \times 10^{-4}$  is above the previous UL of  $1.2 \times 10^{-4}$  obtained by CLEO [1]. It is also considerably higher than the factorization prediction of  $0.7 \times 10^{-4}$  [2]. This could indicate the presence of final state interactions, or other corrections to factorization. It is customary to decompose [2] the  $B^- \rightarrow D^0\pi^-$  and  $\bar{B}^0 \rightarrow D^+\pi^-$ ,  $D^0\pi^0$  decay amplitudes into isospin  $\frac{1}{2}$  and  $\frac{3}{2}$  components. Our measurement of  $\mathcal{B}(\bar{B}^0 \rightarrow D^0\pi^0)$ , together with the known branching fractions [8] of the other two modes, suggest a rescattering phase difference between isospin  $\frac{1}{2}$  and  $\frac{3}{2}$  amplitudes that is  $31^\circ \pm 7^\circ$ . A similar value,  $32^\circ \pm 8^\circ$ , is obtained for the  $\bar{B} \rightarrow D^*\pi$  system.

Our measurements of  $\mathcal{B}(\overline{B}^0 \rightarrow D^0\eta) = (1.4^{+0.5}_{-0.4} \pm 0.3) \times 10^{-4}$  and  $\mathcal{B}(\overline{B}^0 \rightarrow D^0\omega) = (1.8 \pm 0.5^{+0.4}_{-0.3}) \times 10^{-4}$  are also higher than the factorization predictions of  $0.5 \times 10^{-4}$  and  $0.7 \times 10^{-4}$  [2]. The central values of the two less significant modes show the same pattern. The results for these modes cannot be accommodated by the aforementioned elastic rescattering phase.

In summary, using 23.1 million  $B\overline{B}$  events collected with the Belle detector, we report the first observations of color-suppressed  $\overline{B}^0 \rightarrow D^0\pi^0$ ,  $D^{*0}\pi^0$ ,  $D^0\eta$ , and  $D^0\omega$  decays, and evidence for  $\overline{B}^0 \rightarrow D^{*0}\eta$  and  $D^{*0}\omega$  modes. All these modes have similar branching fractions with central values between  $1.4 \times 10^{-4}$  and  $3.1 \times 10^{-4}$ , as given in Table I. They are all consistently higher than recent theoretical predictions based on the factorization hypothesis. This may be accounted for by additional corrections to the factorization models, or by non-factorizable effects such as final state interactions.

We wish to thank the KEKB accelerator group for the excellent operation of the KEKB accelerator. We acknowledge support from the Ministry of Education, Culture, Sports, Science, and Technology of Japan and the Japan Society for the Promotion of Science; the Australian Research Council and the Australian Department of Industry, Science and Resources; the Department of Science and Technology of India; the BK21 program of the Ministry of Education of Korea and the Center for the High Energy Physics sponsored by the KOSEF; the Polish State Committee for Scientific Research under contract No.2P03B 17017; the Ministry of Science and Technology of Russian Federation; the National Science Council and the Ministry of Education of Taiwan; and the U.S. Department of Energy.



## REFERENCES

- [1] CLEO Collaboration, B. Nemati *et al.*, Phys. Rev. D **57**, 5363 (1998). \*Recent CLEO results, T. E. Coan *et al.*, hep-ex/0110055, submitted to Phys. Rev. Lett., also presented an observation of the  $D^0\pi^0$  and  $D^{*0}\pi^0$  modes.
- [2] See, for example, M. Neubert and B. Stech, in: *Heavy Flavours II*, ed. A. J. Buras and M. Lindner (World Scientific, Singapore, 1998), pp. 294 [hep-ph/9705292].
- [3] W.S. Hou and K.C. Yang, Phys. Rev. Lett. **84**, 4806 (2000).
- [4] I. Dunietz and A. Snyder, Phys. Rev. D **43**, 1593 (1991).
- [5] Charge conjugate modes are implicitly included throughout the paper.
- [6] Belle Collaboration, A. Abashian *et al.*, KEK Progress Report 2000-4 (2000), to appear in Nucl. Inst. and Meth. A.
- [7] KEKB B Factory Design Report, KEK Report 95-7 (1995), unpublished.
- [8] Particle Data Group, D. E. Groom *et al.*, Eur. Phys. J. C **15**, 1 (2000).
- [9] R. A. Fisher, Annals of Eugenics, **7**, 179 (1936).
- [10] E. Farhi, Phys. Rev. Lett. **39**, 1587 (1977).
- [11] CLEO Collaboration, R. Ammar *et al.*, Phys. Rev. Lett. **71**, 674 (1993).
- [12] Belle Collaboration, K. Abe *et al.*, Phys. Lett. B. **517**, 309 (2001)
- [13] G. C. Fox and S. Wolfram, Phys. Rev. Lett. **41**, 1581 (1978).
- [14] CLEO Collaboration, J. Alexander *et al.*, Phys. Rev. **D64**, 092001 (2001)
- [15] J. E. Gaiser *et al.*, Phys. Rev. D **34**, 711 (1986).

TABLE I. The obtained signal yields, statistical significances ( $\Sigma$ ), background events from generic  $B\bar{B}$  decays ( $B\bar{B}$  bg),  $D^{*0}h^0$  feed-down ( $D^{*0}h^0$ ), and  $q\bar{q}$  production ( $q\bar{q}$  bg), reconstruction efficiencies ( $\epsilon$ ) (including the sub-decay branching fractions), branching fractions ( $\mathcal{B}$ ), and 90% confidence level upper limits (UL) for  $\bar{B}^0 \rightarrow D^{*0}\eta$  and  $D^{*0}\omega$  are listed together with the theoretical predictions (Th) [2]. The background events are estimated under the signal peak (in the region of  $-0.1 \text{ GeV} < \Delta E < 0.1 \text{ GeV}$ ).

Mode	Signal Yield	$\Sigma$	$B\bar{B}$ bg	$D^{*0}h^0$	$q\bar{q}$ bg	$\epsilon(\%)$	$\mathcal{B} (\times 10^{-4})$	UL ( $\times 10^{-4}$ )	Th ( $\times 10^{-4}$ )
$D^0\pi^0$	$126.2^{+16.1}_{-15.5}{}^{+7.2}_{-5.2}$	9.3	26.7	1.3	145.6	1.79	$3.1 \pm 0.4 \pm 0.5$	–	0.7
$D^{*0}\pi^0$	$26.4^{+7.7}_{-7.1}{}^{+1.6}_{-2.2}$	4.1	5.9	–	10.4	0.42	$2.7^{+0.8}_{-0.7}{}^{+0.5}_{-0.6}$	–	1.0
$D^0\eta^*$	$22.1^{+7.0}_{-6.3}{}^{+2.0}_{-1.8}$	4.2	3.4	0.7	19.1	0.67	$1.4^{+0.5}_{-0.4} \pm 0.3$	–	0.5
$D^{*0}\eta$	$7.8^{+3.6}_{-3.0} \pm 0.7$	3.3	1.4	–	1.5	0.17	$2.0^{+0.9}_{-0.8} \pm 0.4$	4.6	0.6
$D^0\omega$	$32.5^{+9.4}_{-8.6}{}^{+4.0}_{-3.1}$	4.4	$5.3(2.3)^\dagger$	1.4	58.5	0.80	$1.8 \pm 0.5^{+0.4}_{-0.3}$	–	0.7
$D^{*0}\omega$	$16.1^{+6.8}_{-6.0} \pm 2.4$	3.0	$5.3(1.5)^\dagger$	–	13.8	0.23	$3.1^{+1.3}_{-1.1} \pm 0.8$	7.9	1.7

\* For decay modes with  $\eta$  mesons, about 70% of the signal is reconstructed in the  $\gamma\gamma$  channel and the remainder is in the  $\pi^+\pi^-\pi^0$  channel.  $^\dagger$  The values in parentheses are the estimated background from  $B^- \rightarrow D^{(*)0}\rho'^-$  decays.

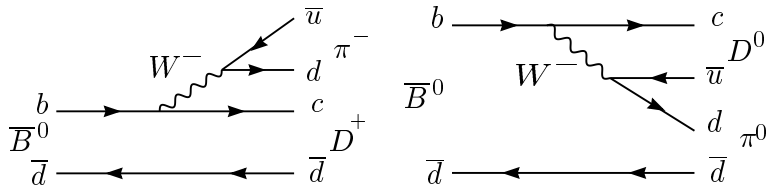


FIG. 1. The external (left) and internal (right) spectator diagrams for  $\bar{B} \rightarrow D\pi$  decays.

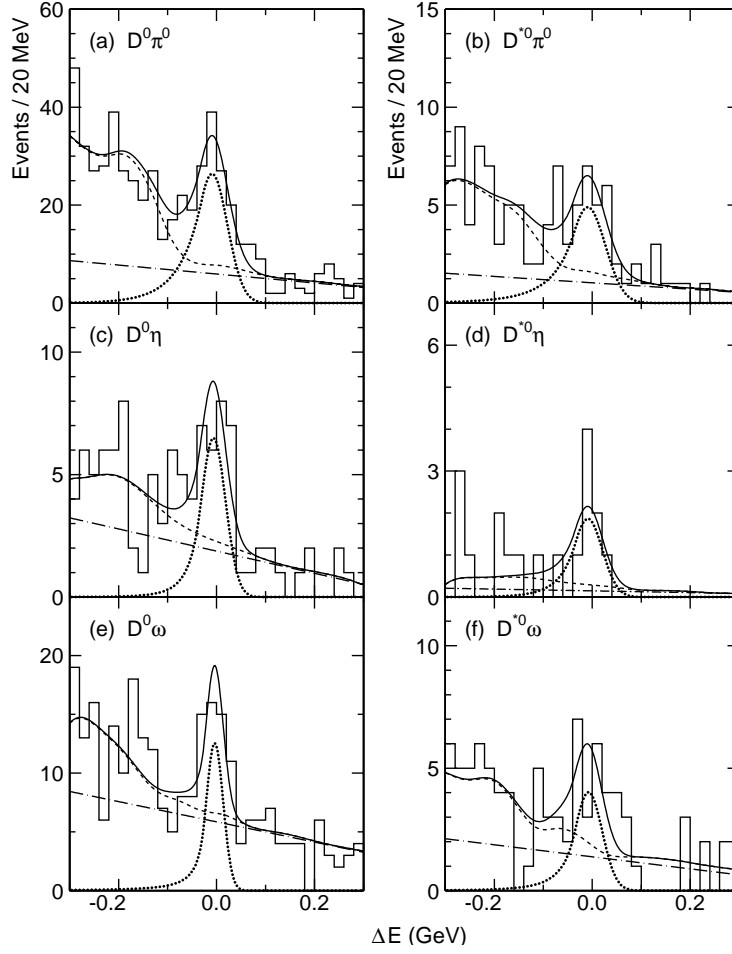


FIG. 2. The  $\Delta E$  distributions for (a)  $D^0 \pi^0$ , (b)  $D^{*0} \pi^0$ , (c)  $D^0 \eta$ , (d)  $D^{*0} \eta$ , (e)  $D^0 \omega$ , and (f)  $D^{*0} \omega$ . The solid lines show the fit results, the dotted lines are the signals, and the dashed lines show the sum of the feed-across and the combinatorial background, with the latter shown separately as the dash-dotted lines.